Fluorescence based fibre optic pH sensor for the pH 10 - 13 range suitable for corrosion monitoring in concrete structures

T. Hien Nguyen[a,1]*, Thillainathan Venugopala[a], Shuying Chen[a], Tong Sun[a], Kenneth T.V. Grattan[a], Susan E. Taylor[b], P. A. Muhammed Basheer[b] and Adrian E. Long[b]

[a]School of Engineering and Mathematical Sciences, City University London, London EC1V 0HB, UK
[b]School of Planning, Architecture and Civil Engineering, Queen's University Belfast, Belfast BT9 5AG, UK

[1]Present address: Organic Semiconductor Centre, University of St Andrews, St Andrews KY16 9SS, UK

Email: thn@st-andrews.ac.uk,   Tel :+44(0)1334461604, Fax : +44(0)1334463104

Abstract:

The design, development and evaluation of an optical fibre pH sensor for monitoring pH in the alkaline region are discussed in detail in this paper. The design of this specific pH sensor is based on the pH induced change in fluorescence intensity of a coumarin imidazole dye which is covalently attached to a polymer network and then fixed to the distal end of an optical fibre. The sensor provides a response over a pH range of 10.0 – 13.2 with an acceptable response rate of around 50 minutes, having shown a very good stability over a period of longer than 20 months thus far. The sensor has also demonstrated little cross-sensitivity to ionic strength (IS) and also excellent photostability through a series of laboratory tests. These features make this type of sensor potentially well suited for *in-situ* long term monitoring of pH in concrete structures, to enhance structural monitoring in the civil engineering sector.

Keywords: Optical fibre sensor, fluorescent sensor, pH sensor, high pH values, corrosion monitoring, coumarin dye.

1. Introduction

Reinforced concrete structures make up a large portion of the physical infrastructure of the world and are of great economic importance in every industrialized nation. The structures of reinforced concrete are usually exposed to a wide variety of damaging influences that leads to reduction in the strength, utility and aesthetic quality of structures[1, 2]. Aside from mechanical stress, corrosion due to chemical and environmental attacks is one of the most damaging processes in concrete[3-5] causing great concern for civil and structural engineers. It presents a safety risk both to people and the environment because significant failure often occurs without prior indication. Corrosion is also a critical economic issue because of the elevated cost of repairing highly damaged structures. In addition to moisture and chloride contents, the pH value is a chemical parameter of major importance for health monitoring of steel-reinforced

concrete structures[3, 6, 7]. A concrete structure exhibits a pH value of about 12.5 to 13.5 at an early age[8]. After a certain period of time, its pH value decreases to a value close to 9.5 as a result of an externally influenced carbonation process. The lifetime of a steel-reinforced concrete structure depends strongly on its internal pH as embedded steels in concrete structures are only passivated at pH values higher than 10[9]. Therefore, monitoring of pH in the range from 10 to 13 is extremely important for prediction and early detection of corrosion condition.

Over the years, in order to improve the quality of the monitoring process and to minimize periodical inspections which are usually expensive, time-consuming and in some cases destructive, several systems for *in-situ*, non-destructive and cost-effective monitoring have been developed. However, the most commonly used approach relies on the electrochemical method [6, 10-14], which has the major inconvenience (and at times impossibility of) prior electrode installation as well as inherent problems associated with the technique such as electrode failures, low sensitivity, and most important ambiguity in the causes of the impedance change. The fibre optic approach used in this work provides an innovative and potentially simpler alternative to its electrochemical counterpart for corrosion monitoring, due to the advantages offered in terms of small size, immunity to electromagnetic interference, remote sensing capability and resistance to chemicals[15, 16]. Most pH optrodes (the optical fibre analogue of electrode) function through monitoring the changes in the absorbance or fluorescence properties of certain pH sensitive indicators which are immobilized on/in proton-permeable solid substrates[17].

Although there have been a number of reports on the development of fibre-optic pH sensors in the literature over the last two to three decades, most of them were constructed to operate, with certain limitations, in the physiological or near neutral pH region. Only a few optrodes have been reported for use in either the low or high pH region where the pH response of most glass pH electrodes is imperfect[18, 19]. The reasons for limited success with many previous designs are quite varied but the use of appropriate pH indicators, the choice of solid substrates and the effective immobilization of the indicators to the substrates are probably the key factors in the development of an optimum optical pH sensor, as they govern the lifetime and signal stability of the sensor, and often have not been achieved in previous designs. It is even more challenging to develop optrodes for monitoring pH changes in concrete as in addition to the requirement for the sensor to be able to measure pH values in the range of 10 – 13 with a resolution of at least 0.5 pH units, the following requirements have to be fulfilled: (i) the sensor has to show long-term stability under strongly alkaline conditions, (ii) the sensor design has to sustain embedment procedure under harsh working conditions and (iii) the sensing element has to be allowed for an intimate contact with the concrete matrix to see pH changes. Several attempts have been made to produce fibre optic pH sensor systems for concrete monitoring but most of them suffer from certain drawbacks in light of their potential practical applications in the field such as poor and inconsistent response[14, 20], drifting of the signal resulting from dye leaching[21], short life span[21], or simply not being able to operate effectively at pH above 12[22].

In this work, a new approach is taken for the development of a pH sensing system in an attempt to overcome the limitations of previous sensors, thus creating more stable, robust and durable and therefore more useful devices. A novel pH sensitive

fluorescent polymer bearing imidazolyl groups was designed, synthesized and used as the sensing element. The protonation/deprotonation of the nitrogen on the imidazolyl groups allows for the determination of pH in the alkaline region of the pH scale. The fluorescence detection method was employed rather than the simpler commonly used method based on colorimetric measurements as fluorescent sensors are usually more precise, having less interference from the light source, and offer higher sensitivity than their colorimetric counterparts[23, 24]. Significantly, attention in the development process was also paid to the mechanical design of the sensor to ensure safe embedment in harsh and corrosive environments.

2. Materials and methods

2.1. General
All chemicals were of analytical grade, purchased from Sigma-Aldrich and were used without further purification. All solvents used were of HPLC grade from Fisher Scientific. All aqueous solutions were prepared using distilled deionized water. ^{1}H and ^{13}C NMR spectra were recorded on a Bruker Avance 500 spectrometer. Mass spectra were run by electron ionisation (EI) mode on a Thermo Finnigan MAT900xp mass spectrometer. IR spectra were recorded on a Bruker Alpha Fourier Transform Infrared Spectrophotometer and were run neat. Melting points were recorded using a Stuart SMP30 melting point apparatus and were uncorrected. Elemental analyses were carried out at the Microanalytical Laboratory, Department of Chemistry at University College London. Absorption and fluorescence measurements of aqueous solutions containing fluorophores were carried out on a PerkinElmer Lambda 35 spectrophotometer and a Horiba Jobin Yvon Fluoromax-4 spetrofluorometer system with FluorEssence^{TM} as driving software, respectively. Refractive indices were measured on an Abbe refractometer. Quantum yields of fluorescence were determined using quinine sulfate as the standard ($\Phi = 0.55$)[25, 26].

2.2. Synthesis of the fluorescent dyes
3-*N*-(Carbethoxy)aminophenol (1): 1 was prepared similarly to the method reported in literature[27]. To a two necked flask equipped with a condenser and a septum were added 3- aminophenol (10.9 g, 100 mmol) and EtOAc (40 mL). The mixture was heated to reflux for 30 min. Ethyl chloroformate (5.4 g, 4764 μL, 50 mmol) was added via syringe over a 10 min period. The reaction mixture was left stirred for a further 20 min then allowed to cool to room temperature to form a white precipitate. The precipitate was removed by filtration and washed with EtOAc (50 mL) and petroleum ether (50 mL). The combined filtrate was concentrated to give **1** as an off-white solid which was further purified by recrystallization from toluene to afford **1** (8.4g, 93%) as white crystals, mp 92 ^{o}C [lit. mp 94-95 ^{o}C (benzene/cyclohexane)]; IR (neat) v_{max} (cm^{-1}) 3294 (NH), 1684 (C=O), 1556, 1449, 1249, 1061; ^{1}H-NMR (500 MHz, CDCl$_3$) δ(ppm): 7.35 (s, 1H), 7.13 (t, 1H, $J = 8.08$), 6.69 (s, 1H), 6.64 (m, 1H), 6.57 (m, 1H), 6.33 (m, 1H), 4.23 (q, 2H, -CH$_2$-, J=7.12 Hz), 1.30 (t, 3H, -CH$_3$, $J = 7.12$); MS (EI): Calcd. m/z = 181.07334 (C$_9$H$_{11}$O$_3$N). Found m/z = 181.07296 (M$^+$).
4-Chloromethyl-7-*N*-(Carbethoxy)aminocoumarin (2): H$_2$SO$_4$ (80%, 40 mL) was pre-cooled in an ice bath. **1** (1.8 g, 10 mmol) was added, followed by ethyl 4-chloroacetoacetate (2.3 g, 1906 μL, 14 mmol) in portions. The mixture was stirred at room temperature under Ar for 19 h, after which it was poured into ice-water (50 mL) and left stirred for a further 30 min. The white precipitate formed was filtered, washed with H$_2$O and recrystallized from EtOH to afford **2** (2.0 g, 71%) as fine needles, mp

242 ^{o}C (decomp.) [lit.[28] mp 247 ^{o}C (MeOH)]; IR (neat) v_{max} (cm^{-1}) 3280 (NH), 3084, 2992, 2929, 1704 (C=O), 1619, 1588, 1520, 1404, 1332, 1204, 1075; ^{1}H-NMR (500 MHz, CDCl$_3$) δ(ppm): 7.59 (d, 1H, H5, $J_{5,6}$=8.7 Hz), 7.50 (d, 1H, H8, $J_{8,6}$=2.14 Hz), 7.36 (dd, 1H, H6, $J_{6,5}$=8.7 Hz, $J_{6,8}$=2.14), 6.82 (s, 1H, NH), 6.45 (s, 1H, H3), 4.65 (s, 2H, -CH$_2$Cl), 4.27 (q, 2H, OCH$_2$-, J = 7.13), 1.34 (t, 3H, -CH$_3$, J = 7.13); MS (EI): Calcd. m/z = 281.04494 (C$_{13}$H$_{12}$O$_4$NCl). Found m/z = 281.04550 (M$^+$).

4-Chloromethyl-7-aminocoumarin (3): 2 (563.4 mg, 2 mmol) was suspended in a mixture of concentrated H$_2$SO$_4$ (1.7 mL) and glacial acetic acid (1.7 mL). The mixture was heated to 125 ^{o}C for 2h. After cooling to room temperature, the yellow solution was poured into H$_2$O and a voluminous precipitate was formed. 4 M NaOH aqueous solution was added to the mixture to bring pH to ~ 9. The yellow precipitate was filtered, washed with H$_2$O, dried *in vacuo* to afford **3** (366 mg, 87%) as a pale yellow solid which was used for synthesis without further purification, mp 182 ^{o}C [lit.[28] mp 187 ^{o}C]; IR (neat) v_{max} (cm^{-1}) 3445 (NH$_2$), 3352 (NH$_2$), 1686 (C=O), 1601 (NH$_2$), 1548, 1404, 1263, 1210, 1145; ^{1}H-NMR (500 MHz, DMSO) δ(ppm): 7.47 (d, 1H, H5, $J_{5,6}$=8.7 Hz), 6.58 (dd, 1H, H6, $J_{6,5}$=8.7 Hz, $J_{6,8}$=2.00), 6.43 (d, 1H, H8, $J_{8,6}$=2.00 Hz) 6.19 (s+s, nonres., 3H, -NH$_2$ + H3), 4.86 (s, 2H, -CH$_2$Cl); MS (EI): Calcd. m/z = 209.02381 (C$_{10}$H$_8$O$_2$NCl). Found m/z = 209.02417 (M$^+$).

7-amino-4-((2-methyl-4-nitro-1*H*-imidazol-1-yl)methyl)-coumarin (4): NaH in mineral oil (60%, 60 mg) was added to a solution of 2-methyl-4-nitroimidazole (203 mg, 1.6 mmol) in DMF (6 mL). The mixture was heated to 100 ^{o}C for 10 min and then cooled down to 60 ^{o}C, after which **3** (314 mg, 1.5 mmol) dissolved in DMF (6 mL) was added. The reaction mixture was left stirring at the same temperature for 18 h then poured into ice. The yellow precipitate formed was collected by filtration, washed with water and recrystallised from EtOH to afford **4** (390 mg, 87%)   as yellow fine crystals, mp 298-300 ^{o}C (decomp.); IR (neat) v_{max} (cm^{-1}) 3430 (NH$_2$), 3324 (NH$_2$), 3221, 3144, 1695 (C=O), 1595 (NH$_2$), 1542, 1498, 1402, 1328, 1290, 1132; ^{1}H-NMR (500 MHz, DMSO) δ(ppm): 8.37 (s, 1H, 5-H-imidazole), 7.44 (d, 1H, H5, $J_{5,6}$=8.69 Hz), 6.61 (dd, 1H, H6, $J_{6,5}$=8.69 Hz, $J_{6,8}$=2.14), 6.45 (d, 1H, H8, $J_{8,6}$=2.14 Hz) 6.27 (s, 2H, -NH$_2$), 5.51 (s, 2H, -CH$_2$-), 5.05 (s, 1H, H3), 2.31 (s, 3H, -CH$_3$); ^{13}C-NMR (DMSO) δ(ppm): 160.7 (C2), 155.9 (C9), 154.0 (C7), 151.1 (4-C-imidazole), 146.1 (C4), 125.7 (C5), 123.1 (5-C-imidazole), 111.7 (C6), 106.2 (C10), 104.5 (C3), 99.0 (C8), 46.6 (-CH$_2$-), 12.8 (-CH$_3$); MS (EI): Calcd. m/z = 300.08531 (C$_{14}$H$_{12}$O$_4$N$_4$). Found m/z = 300.08584 (M$^+$); Elem. Anal. Calcd. for C$_{14}$H$_{12}$O$_4$N$_4$ (300.27): C 56.00 , H 4.03, N 18.66. Found: C 56.72 , H 4.50, N 18.19.

7-(4-vinylbenzylamino)-4-((2-methyl-4-nitro-1*H*-imidazol-1-yl)methyl)-coumarin (5):

A mixture of **4** (300 mg, 1 mmol), vinylbenzylchloride (155 μL, 168 mg, 1.1 mmol, 1 mmol), potassium carbonate (401 mg, 2.9 mmol), posstasium iodide (49 mg, 0.3 mmol) in dry MeCN (20 mL) was heated under argon at 80 ^{o}C for 2 days. After cooling to room temperature, H$_2$O was added to dissolve the inorganic salts. The mixture was filtered to remove insoluble materials. EtOAc was then added. The organic phase was washed with H$_2$O (2 x 50 mL) and saturated aqueous NaCl (50 mL), dried over MgSO$_4$, filtered, and concentrated *in vacuo*. The resulting orange-red residue was chromatographed on silica gel using CH$_2$Cl$_2$-EtOAc (4:6, v/v) as eluent to give an orange solid which was further purified by recrystallisation from ethanol to afford **5** (40 mg, 10 %) as a yellow-orange solid, mp 194 ^{o}C; IR (neat) v_{max} (cm^{-1}) 3335 (NH), 3144, 1694 (C=O), 1601, 1540, 1500, 1404, 1321, 1291, 1148; ^{1}H-NMR (500 MHz, CDCl$_3$) δ(ppm): 7.69 (s, 1H, 5-H-imidazole), 7.41 (d, 2H, aromaticH J=8.13 Hz), 7.30 (d, 2H, aromaticH J=8.15 Hz), 7.20 (d, 1H, H5, $J_{5,6}$=8.72 Hz), 6.71

(dd, 1H, C$\textbf{\textit{H}}$=CH$_2$, J=10.91 Hz, J=17.60 Hz), 6.57 (dd, 1H, H6, $J_{6,5}$=8.72 Hz, $J_{6,8}$=2.36 Hz), 6.53 (d, 1H, H8, $J_{8,6}$=2.32 Hz), 5.75 (d, 1H, CH=C$\textbf{\textit{H}}_a$H$_b$ J=17.61 Hz), 5.43 (s, 1H, H3), 5.26 (d, 1H, CH=CH$_a\textbf{\textit{H}}_b$,J=10.90 Hz), 5.17 (s, 2H, C4C$\textbf{H}_2$-), 4.85 (t, 1H, -NH-, $J_{\text{NH-CH2}}$ = 5.52 Hz), 4.41 (d, 2H, CH$_2$NH-, $J_{\text{CH2-NH}}$ = 5.55 Hz), 2.44 (s, 3H, -CH$_3$); ^{13}C-NMR (CDCl$_3$) δ(ppm): 156.3 (C2), 155.0 (2-C- imidazole), 154.0 (C9), 147.7 (C7), 141.1 (C4), 140.0 (4-C-imidazole), 137.3 ($\textbf{\textit{C}}$CH$_2$NH-), 136.2 ($\textbf{\textit{C}}$H=CH$_2$), 128.0 (($\textbf{\textit{C}}$CH=CH$_2$), 127.6 (aromaticC), 126.8 (aromaticC), 123.7 (C5), 119.9 (5-C-imidazole), 114.8 (CH=$\textbf{\textit{C}}$H$_2$), 107.6 (C3), 107.1 (C10), 99.1 (C8), 47.5 (-$\textbf{\textit{C}}$H$_2$NH-), 46.9 (C4$\textbf{\textit{C}}$H$_2$-), 13.1 (-CH$_3$); MS (EI): Calcd. m/z = 416.14791 (C$_{23}$H$_{20}$O$_4$N$_4$). Found m/z = 416.14827 (M$^+$); Elem. Anal. Calcd. for C$_{23}$H$_{20}$O$_4$N$_4$ (416.43): C 66.34 , H 4.89, N 13.45. Found: C 65.76 , H 4.66, N 12.89.

2.3. pH probe design and fabrication

The next step in the development of the sensor was the creation of an appropriate pH sensing probe incorporating the dye developed. This requires a multi-step process, as described below:

Preparation of the polymer: 7-(4-vinylbenzylamino)-4-((2-methyl-4-nitro-1H-imidazol-1-yl)methyl)-coumarin (**5**) (20.8 mg, 0.05 mmol), methacrylic acid (8.6 mg, 8.5 µL, 0.1 mmol), 1,4-bis(acryloyl)piperrazine (97,1 mg, 0.5 mmol) and pluronic P84 (84 mg) were weighed into a borosilicate glass vial and dissolved in dimethylformamide (500 µL). Azobis(isobutyronitrile) (AIBN) (5 mg) was then added. The vial was placed in a sonicating water bath until AIBN was fully dissolved, then purged thoroughly with argon for about 2 min before being tightly capped and sealed. Polymerisation was carried out at 80 ^{o}C in the dark for approximately 20 h. The resulting hard bulk polymer was then hand ground with a mortar and pestle until fine particles were obtained. The polymer particles were washed to remove unreacted materials by repeated incubation in MeOH (50 mL solvent each), centrifugation and re-suspension (4×0.5h incubations), followed by the same procedure with H$_2$O (2×0.5 h incubations) and finally on a sintered filter with MeOH (50 mL). After washing, polymer particles were dried in vacuum and stored in the dark until use.

The sensing tablet was prepared by holding a layer consisting of 4 mg of polymer particles in between a quartz disc (6 mm dia.) and a nylon membrane (20 µm pores, GE). The layer was kept in place by an O-ring as shown in Fig.1.

The tablet with the quartz disc side facing upward was then put in a holder made from Polytetrafluoroethylene (PTFE) and specifically for this work with a SMA thread on the top to enable its connection to the fibre using a SMA connector. The porous bottom of the tablet enables the direct contact between the sensing tablet and the surrounding environment. All the parts were kept tightly together by placing a thin layer of super glue over the joints.

2.4. Experimental set-up

With the probe having been fabricated as described above, it was necessary to calibrate the sensor prior to its use in the applications domain. The set-up used for the measurements undertaken to calibrate the probe is as presented in Fig. 1, where light from a 3 mW LED (Roithner Lasertechnik), emitting at a center wavelength of 375 nm is coupled through a multimode UV/Visible fiber (with hard polymer cladding, 1000µm silica core and numerical aperture NA of 0.37, Thorlabs), using collimation and focusing lenses (Comar), into one branch of a 2x1 multimode fiber coupler (Ocean Optics). The other end of the fibre coupler is connected, through a SMA connector, to the sensor probe with the sensing tablet being located at the bottom.

Following pH interaction with the active region, a portion of the total light emitted from the sensing element is collected and guided through the other branch of the fiber coupler to an Ocean Optics USB2000 spectrometer, with the output being displayed on a computer screen.

2.5. Principle of pH measurement based on fluorescence intensity and pK_a calculation

The development of the present pH optrode is basically based on the fluorometric determination of pH. As stated above, it makes use of the coumarin dye as fluorescent indicator, HA, to induce pH sensitive changes in the measured fluorescence intensity. In aqueous solution, the following equilibrium can be reached:

$$HA \leftrightarrow H^+ + A^-$$

The relationship between the protonation state of the indicator and the pH is governed by the Henderson-Hasselbalch equation:

$$pH = pK_a + \log \frac{[A^-]}{[HA]} \quad (1)$$

where $[A^-]$ and [HA] are the concentrations of the dissociated and undissociated forms of the indicator and pK_a is the acid-base constant. $[A^-]$ and [HA] are related to fluorescence intensities by $[A^-] = F - F_{max}$ and $[HA] = F_{min} - F$ where F is a measured fluorescence intensity of the system, F_{max} is the fluorescence intensity of the fully protonated system and F_{min} is the fluorescence intensity of the deprotonated system. The expressions are then substituted into Equation 1 to provide Equation 2.

$$pH = pK_a + \log \frac{F - F_{max}}{F_{min} - F} \quad (2)$$

Equation 2 can be re-written in terms of F to give

$$F = \frac{F_{max} + F_{min} \times 10^{(pH - pK_a)}}{10^{(pH - pK_a)} + 1} \quad (3)$$

This results in an 'S-shaped' relation of the fluorescence intensity versus pH graph, centered on the pK_a value. Equation 3 is used as a model for a nonlinear fitting method to calculate the pK_a values for the free dyes, which is the pH where 50% of the dye population in solution is protonated.

The pK_a value calculation for the polymer-bound dye was performed using the Boltzmann model – Equation (4) where dpH is the slope of the curve within its linear zone.

$$F = \frac{F_{max} + F_{min} \times e^{(pH - pK_a)/dpH}}{e^{(pH - pK_a)/dpH} + 1} \quad (4)$$

Insert figure 1 here

3. Results and discussion

3.1. Choice of indicator, solid support and immobilisation method

Although there have been a variety of pH indicators, both commercially available including azo dyes[8, 18, 32-34], trinitrobenzensulfonic acid[14], thymol blue[20, 21, 35, 36], cresol red[20], phenolphthalein[19], aniline blue[37], rhodamine 19[38], Victoria blue[39] etc. as well as reported in the literature such as fluorescent Schiff bases[40], porpholactones[41] or a benzo[de]anthracen-7-one derivative[23] , that are known to be useful for the spectroscopic determination of high pHs, the majority of them are absorptive dyes rather than fluorescent dyes and only a few meet the requirements of being stable for a long period of time in highly alkaline media, possessing a pK_a in the range between 11-12.5, having reasonable fluorescence quantum yield and good photostability, being fully compatible with LED light sources and bearing one or more functional chemical groups suitable for covalent immobilization of the indicator. It was therefore decided to synthesize the sensitive dye needed for the application considered rather than to use an 'off-the-shelf' indicator. Coumarin based indicators have been chosen for this application as coumarins are widely used as laser dyes for single-molecule fluorescence and so they are 'tried and tested' in terms of the key property of being photo-stable[42, 43]. It has also been reported that a coumarin with an imidazole substituent shows response to pH in the alkaline region due to the protonation/deprotonation of the nitrogen on the imidazolyl group[44]. The design of the indicator dye was tailored based on this core structure and suitable functional group(s) for immobilization of the indicator to a substrate.

Having created an appropriate indicator dye, it is equally important to perform an effective immobilization of the dye to a suitable solid substrate. Prior work has shown that poor immobilization results in dye leaching and consequently a drifting of the calibration of the probe, which leads to the gradual breakdown of its useful sensing ability[17]. Among several widely used immobilization methods are included absorption or entrapment[45-47], layer-by-layer (LbL) electrostatic self-assembly [48, 49] and covalent binding[18, 50-53]. The first two approaches are generally easier and simpler but not suitable for this type of application as they suffer from numerous disadvantages such as cracking, dye leaching and inhomogeneity of the material (in case of absorption or entrapment in a sol-gel matrix) or irreversible damage at extreme pH values and issue related to effect of ionic strength (in case of electrostatic attachment). The covalent binding method can produce more reliable and durable sensors, as the indicators are virtually bonded to the substrate therefore they are unlikely to leach out under normal conditions, although the fabrication process is relatively complicated and time-consuming [54].

Regarding solid supports, various materials have been employed as the supports for dye immobilization including cellulose membrane[18, 33, 50, 55], silica sol-gels[56, 57] and synthetic organic polymers[32, 53] with cellulose and sol-gels being more commonly used than the other due to the optical transparency of their matrices and in many cases, the convenience of attachment process. However, cellulose degrades easily in highly alkaline media[32, 58] and sol-gels are completely deteriorated at pH higher than 10 within relatively short time. Therefore, they are not suitable for this type of sensor, leaving synthetic polymers the favourable option. The indicator dye can be connected into polymer matrix by either co-polymerisation of the dye monomer and appropriate co-monomer(s) or by attaching the reactive dye to a readily prepared polymer. In this work, the former method was used because it is easier to

design different polymer matrices and control their properties to meet the requirements of the sensor in terms of polymer rigidity, hydrophilicity and optical density by using different mixtures of co-monomers.

3.2. Synthesis of polymerisable fluorescent dyes

To meet the desired requirements discussed above, the fluorescent dye used in this work was designed to include a polymerisable group and the coumarin core structure with an imidazole substituent. The linkage between the polymerisable group and the coumarin should be stable enough to sustain strongly alkaline media. A novel polymerisable coumarin, vinylbenzylamino imidazolylmethyl coumarin (**VIC**, **5**), was prepared in multiple steps starting from a commercially available phenolic compound as outlined in Scheme 1. The Pechmann reaction of a phenol with a β-carbonyl ester is a versatile approach for the synthesis of 4-substituted coumarins. **2** was prepared similarly to the method reported in the literature[28]. The substitution of chlorine for an imidazolyl group was achieved by performing a reaction with 2-methyl-4-nitroimidazole, following the method described by Al-Soud *et al.* [59]. A polymerisable groups was introduced into the coumarin structure by reacting the amine substituted coumarin **4** with 4-vinylbenzylchloride to give the secondary amine **5**.

Insert scheme 1 here

The stability of the synthesized indicator dye to OH⁻ attack was tested over a period of about 2 months by dissolving an exact amount of the dye in a minimum volume of MeOH (the dye is not soluble in water). The solution was then diluted 1 in 50 with 0.1 M NaOH in a plastic container and left under ambient conditions. The container was closed to avoid evaporation and wrapped with aluminum foil to prevent light from getting to the solution. No other special precaution was taken to preserve the indicator. Samples were collected at regular time intervals and fluorescence and absorption spectra were recorded in comparison to a freshly prepared solution. The measurements showed no difference between the stored solution and the freshly prepared solution throughout the period, suggesting that any degradation of the dye was either insignificant, or the degraded products did not affect the absorption and fluorescence properties of the indicator.

3.3. Spectral properties and pK_a values of free indicators in solution

In neutral aqueous solution (with the addition of 1.5% EtOH to solubilize the compound), the absorption spectrum of **VIC** (**5**) shows only one main absorption band in the UV region, at 370 nm (Fig. 2). Emission spectrum for the compound recorded in the same solvent using excitation at the absorbance maximum includes one band at 470 nm. The red-shifted fluorescence and absorbance of **VIC** with respect to other coumarins may be due to the conjugation of the lone-pair electrons of the amine nitrogen at the 7 position with the π system. It is also noted that **VIC** exhibits a very large Stokes shift (the difference in wavelength between the absorption and the fluorescence spectral peaks) of 100 nm, which is very important for the sensor system design to minimize the interference of the excitation light with the fluorescence emission.

Insert figure 2 here

Insert table 1 here

In aqueous solution, the dye shows a decrease in fluorescence intensity with increasing pH in the alkaline region. This can be attributed to the equilibrium between the protonated and deprotonated forms of the imidazolyl nitrogen as shown in Scheme 2. The protonated form is fluorescent and the deprotonated form is much less so. Therefore, the fluorescence intensity of the dye is lower at higher pH values. It has been proposed that the difference in fluorescence intensity between two forms is due to photoinduced electron transfer (PET) between the imidazole (receptor) and coumarin (fluorophore)[44, 60]. The nitrogen lone pair of electrons quenches the fluorescence of the coumarin through PET. The presence of low concentration of hydrogen ions causes protonation of the nitrogen, resulting in PET from the imidazole to coumarin being hindered and hence the fluorescence intensity increases.

Insert scheme 2 here

To determine the pK_a value for the free dye, a series of pH titration experiments was carried out using 50 mM phosphate buffer solutions with different pH. In the titration, 20 µL of 0.8 mM stock solution of the dye in EtOH was added to 3 mL of buffer in a cuvette, followed by measurement of emission spectra. All samples were prepared in duplicate or triplicate and the data presented were average values. The calculation of the pK_a value was performed based on the fluorescence intensities at a fixed maximum emission wavelength using a nonlinear fitting method according to Equation 3. The data obtained for the dye are summarized in Table 1.

3.4. Polymer preparation and probe fabrication

Polymers were prepared in dimethylformamide (DMF) by free-radical polymerization using azobis(isobutyronitrile) as initiator. These were prepared as monolithic polymers and ground into small particles, since these are easier to produce than spherical beads which can be made by precipitation polymerisation and since a minimal amount of solvent is required. There is no problem with scattering from the irregular-shaped particles because with the coumarin used here the Stokes shift is sufficient that emission can be measured well above the scattered wavelengths. Since the sensor was designed to work in aqueous/moisturous environments, 1,4-bis(acryloyl)piperrazine was used as the cross-linker as it is water soluble, hence producing polymers with a more hydrophilic backbone. Methacrylic acid was included as a co-monomer so that the polymers should not be too rigid and it can also increase the hydrophilicity of the polymers. Pluronic P84 was added to increase the surface area and porosity. It is important that the polymer used has the right molar ratio of cross-linker to monomers since lower cross-linking gives insufficiently robust polymer and higher cross-linking gives too rigid polymer, hence preventing the diffusion of hydrogen ions from surrounding environments to the fluorescent receptor. After trying and testing different ratios in terms of polymer packing (considering the swelling and shrinking factor), response time and the strength of fluorescence signal obtained, it was found that a molar ratio of cross-linker to monomers of about 10:3-4 produced good polymers for this application. The molar amount of fluorescent monomer used was fixed at 1:10 of the cross-linker. More fluorescent monomer would be expected to give a stronger fluorescent signal but too high a concentration of fluorophore could also result in fluorescence quenching by the inner filter effect.

Previous studies demonstrated that covalent immobilisation of a fluorescent dye directly onto the end surface of an optical fibre through a polymerization process of the fluorescent monomer and co-monomers with an optical fibre functionalized with polymerizable groups produced an intrinsic optical fibre sensor with superior performance and fast response[61]. However, for the application in concrete structures, this design is not suitable due to the fragile nature of optical fibres, especially in highly alkaline media. The polymer was, therefore, prepared separately and packed in a tablet form in between a quartz disc and a nylon membrane to provide a robust mechanical design for safe embedment in harsh and corrosive environments.

3.5. Response time of the sensor

Before performing measurements to calibrate the sensor, its response time was investigated. Fig. 3 shows the dynamic response of the sensor obtained from the spectrofluorometer using the same setting to a step change from pH 10 to pH 13 and back again. In general, the response time was rather long and at the initial stage depended on the direction in which the pH of the solution was varied. It took around 10 minutes to obtain 70% of the total signal change for the low to high pH variation whereas the same amount of change for the reverse variation required nearly twice as much time. However, the response time, which in this work is considered to be the time required for 95% of the total signal change, was almost equal in both directions of pH variation and was measured as around 50 minutes. The signal leveled off after equilibrium and no drift in response was observed under the experimental conditions employed. This response time, which is long in comparison with those of previously developed pH sensor systems[38, 39, 61], could be due to diffusion in the rather thick polymer layer. However, this is not a problem for concrete monitoring as pH changes in concrete structures occur over much longer periods of time.

Insert figure 3 here

3.6. Response of the sensor to pH

The calibration measurements of the sensor characteristics were performed in 50 mM phosphate buffer at different pH. They were carried out in duplicate and the data presented were average values. The titration curve is shown in Fig. 4. The sensor probe exhibited a decrease in fluorescence intensity with increasing pH in the range from 10 to 13.2, which conveniently is wider than the dynamic response range of the free dye. Measurements could not be carried out at pH higher than 13.2 as some leaking of the dye was observed at pH 13.5. The pK_a value calculated using Eq. (4) for the probe is 11.9 ± 0.2. This value for the immobilized form of the dye is slightly lower than that for its free form in solution and this arises probably because of the change in the polarity of the microenvironment.

Insert figure 4 here

3.7. Effect of ionic strength (IS)

Sensitivity to IS can be a serious problem in the cases of optical fiber sensors as it affects pK_a values, thus resulting in errors in pH determination. Most optrodes reported in the literature so far suffer from cross-sensitivity to IS to a certain degree, especially those that are based on indicators with charged group(s)[62] or those that make use of sol-gels[57] or cellulose membrane[18] as solid support. The effect of IS

was investigated with the prepared pH 10 and pH 13 phosphate buffer solutions adjusted with NaCl to different ionic strengths ranging from 10 mM to 2000 mM. The fluorescence intensity obtained for each solution was converted to a pH value using the calibration curve and the error was calculated. As can be seen from Fig.5, there appears to be no sensitivity to IS for the sensor at pH 10, even at very high concentrations of NaCl. The insignificant errors caused are probably due to the system error rather than the change in IS. At pH 13, the fluorescence intensity of the sensor decreased slightly with increasing IS, which caused an increase in the calculated pH values with respect to the actual values. Increasing IS from 0 to 2M resulted in an error (increase) of 0.96 pH units. However, the practical ranges of IS in most common media are much lower. In concrete, chloride is the dominant species and its concentration range is usually from 1000 ppm (0.028 M) to as high as 10000 ppm (0.28 M), which is considered the threshold where active corrosion of reinforced steel is initiated. The error caused in this range is maximum 0.35 pH units at pH 13, which is acceptable for concrete monitoring that only requires a resolution of 0.5 pH units.

Insert figure 5 here

3.8. Sensor stability

The stability of the probe both in terms of storage, its susceptibility to error due to intense irradiation of the sample and its reproducibility in use are all very critical to the successful application of the system. An evaluation of these parameters was made in order to understand better the performance of the sensor and establish its suitability for industrial applications. The stability of the sensor was tested by calibrating it with buffer solutions at different pH values ranging from 9.0 to 13.0 and recalibrating it after 1.5 months and then after 20 months. After each calibration, the probe was immersed in a pH 7.0 buffer for a few hours, followed by washing thoroughly with distilled water and then it was stored in dry state in the dark until next use. Before testing the probe again, it was conditioned in a pH 7 buffer solution for one day. The response functions were rather similar. No significant difference was observed between the measurements and the pK_a values calculated, which were found to be 11.95 ± 0.30 (initial calibration), 12.04 ± 0.43 (after 1.5 months) and 11.93 ± 0.16 (after 20 months). The variation in pK_a and drifts in the working function of the sensor over time is small and can be compensated for by recalibration if required.

Insert figure 6 here

3.9. Photostability

Photostability is one of the critical properties of fluorescent indicators and thus of the dye used in this sensor application. In order to test the photostability of the material, the probe was coupled into the fluorimeter through a dichroic mirror using a fiber bundle. The excitation light (at a wavelength of 400 nm) was launched to the distal end of the probe illuminating the sensing material with light from the intense, high power Xe lamp of the fluorimeter continuously for 1 h. The fluorescence intensity data from the probe were collected over that period and displayed. Fig.7 shows the fluorescence intensities of the sensor probes in dry state and in a pH 10 buffer solution as function of time during 60 min of continuous illumination by light from a high power Xe lamp. It was interesting to observe that the intensity of fluorescence

was reduced by 7-8% for the dry state over the time investigated and with the high flux of photons onto the probe. However, under the same conditions, no photobleaching was seen for the similar probe, prepared in exactly the same way using the same polymer, which was immersed in a pH 10 buffer solution. The reason for the difference in photostability between the dry probe and wet probe is unclear. It could be because the excited single state of the dye is stabilised by solvation. It should be noted that in actual measurements, the material is not excited continuously, but only for 30 seconds each time when data need to be collected, after the sensor reaches its equilibrium, by a much weaker 3 mW LED light source. Also, since there is always a certain level of moisture in concrete structures, the sensor is never in a totally dry state when it is embedded in concrete. Therefore, a little photobleaching of the material in dry state when being illuminated by a strong light should not cause any problem for the monitoring. When compared to the results of other materials, this still offers excellent performance: the decrease observed in the fluorescence intensity was 65% for carboxyfluorescein and 10-13% for iminocoumarin derivatives, again after 60 min of continuous illumination using a mercury lamp[24]. Thus an important conclusion is that the material prepared using the coumarin fluorophore and synthesized specifically for this application in this work possesses superior photostability, a feature that is critically important with excitation of sensor probes by high intensity solid state sources.

Insert figure 7 here

4. Conclusions

In this paper, a novel fibre optic sensor system for sensing pH in the alkaline region has been reported. The sensing mechanism was based on the pH induced change in fluorescence intensity of a coumarin imidazole dye which was covalently attached to a polymer network by co-polymerisation of the dye monomer with methacrylic acid co-monomer and 1,4-bis(acryloyl)piperrazine cross-linker. The polymer particles were held in between a quartz disc and a nylon membrane and fixed to the distal end of an optical fibre, which provided a robust and durable mechanical design to ensure safe embedment in harsh and corrosive environments.

Laboratory tests demonstrated that the sensor responded to pH in the range from 10 to 13 and a good stability of the sensor performance has been observed after it has been stored appropriately for a period of 20 months. No sensitivity to IS was observed at pH 10 and only a small degree of that was seen at pH 13, by which errors caused to the calculated pH values with respect to the actual values were within the acceptable range. The probe was also highly photo-stable, showing no photo-bleaching, when immersed in a pH 10 buffer solution, after 60 minutes of continuous illumination using a high power Xe lamp. A further important feature of this type of sensor is that it is potentially inexpensive to produce in quantity and the large Stokes shift shown allows for more accurate measurements due to the minimum level of interference between light source and fluorescence signals generated. Therefore, the sensor system developed is potentially suited for *in-situ* long term monitoring of pH in concrete structures. Tests are currently in progress to evaluate the performance of the sensor when it is embedded in concrete and the results will be reported in the next paper.

References

[1] D. Cusson and B. Isgor, Durability of concrete structures: prevention, evaluation, inspection, repair and prediction, Canadian Civil Eng. 21 (2004) 4-5.

[2] E. Proverbio, Evaluation of deterioration in reinforced concrete structures by AE technique, Materials and Corrosion-Werkstoffe Und Korrosion 62 (2) (2011) 161-169.

[3] P. K. Mehta, Durability - Critical issues for the future, Concrete International 19 (7) (1997) 27-33.

[4] F. Mansfeld, H. Shih, A. Postyn, J. Devinny, R. Islander, and C. L. Chen, Corrosion Monitoring and Control in Concrete Sewer Pipes, Corrosion 47 (5) (1991) 369-376.

[5] A. A. Panova, P. Pantano, and D. R. Walt, In situ fluorescence imaging of localized corrosion with a pH-sensitive imaging fiber, Anal. Chem. 69 (8) (1997) 1635-1641.

[6] M. Kolar, A. Doliska, F. Svegl, and K. Kalcher, Tungsten - tungsten trioxide electrodes for the long-term monitoring of corrosion processes in highly alkaline media and concrete-based materials, Acta Chim. Slov. 57 (4) (2010) 813-820.

[7] M. G. Stewart, X. Wang, and M. N. Nguyen, Climate change impact and risks of concrete infrastructure deterioration, Engineering Structures 33 (4) (2011) 1326-1337.

[8] C. Vimer, S. Yu, and M. Ghandehari, Probing pH levels in civil engineering materials, J. Mater. Civ. Eng. 21 (2) (2009) 51-57.

[9] L. J. Parrott, A Study of Carbonation-Induced Corrosion, Mag. Concrete Res. 46 (166) (1994) 23-28.

[10] G. S. Duffo, S. B. Farina, and C. M. Giordano, Embeddable reference electrodes for corrosion monitoring of reinforced concrete structures, Materials and Corrosion-Werkstoffe Und Korrosion 61 (6) (2010) 480-489.

[11] V. Raman and T. Nishimura, Monitoring of Environmental Factors and Corrosion Analysis of Reinforcing Steel in Mortar, Materials Transactions 50 (4) (2009) 799-805.

[12] G. S. Duffo, S. B. Farina, and C. M. Giordano, Characterization of solid embeddable reference electrodes for corrosion monitoring in reinforced concrete structures, Electrochim. Acta 54 (3) (2009) 1010-1020.

[13] R. G. Du, R. G. Hu, R. S. Huang, and C. J. Lin, In situ measurement of Cl-concentrations and pH at the reinforcing steel/concrete interface by combination sensors, Anal. Chem. 78 (9) (2006) 3179-3185.

[14] R. Srinivasan, T. E. Phillips, C. B. Bargeron, M. A. Carlson, E. R. Schemm, and H. M. Saffarian, Embedded micro-sensor for monitoring pH in concrete structures, Smart Structures and Materials: Smart Systems for Bridges, Structures, and Highways, 2000, pp. 40-44.

[15]   K. T. V. Grattan and B.T.Meggitt, Chemical and Environmental Sensing, in *Optical Fiber Sensor Technology*, vol. 4: Kluwer Academic Publishers, 1999.

[16]   W. J. McCarter and O. Vennesland, Sensor systems for use in reinforced concrete structures, Constr. Build. Mater. 18 (6) (2004) 351-358.

[17]   Z. H. Liu, J. F. Liu, and T. L. Chen, Phenol red immobilized PVA membrane for an optical pH sensor with two determination ranges and long-term stability, Sens. Actuators, B 107 (1) (2005) 311-316.

[18]   T. Werner and O. S. Wolfbeis, Optical sensor for the pH 10-13 range using a new support material, Fresenius J. Anal. Chem. 346 (6-9) (1993) 564-568.

[19]   T. Gotou, M. Noda, T. Tomiyama, H. Sembokuya, M. Kubouchi, and K. Tsuda, In situ health monitoring of corrosion resistant polymers exposed to alkaline solutions using pH indicators, Sens. Actuators, B 119 (1) (2006) 27-32.

[20]   W. G. Xie, T. Sun, K. T. V. Grattan, D. McPolin, P. A. M. Basheer, and A. E. Long, Fibre optic chemical sensor systems for internal concrete condition monitoring,   Second European Workshop on Optical Fibre Sensors: Proceedings, 2004, pp. 334-337.

[21]   P. A. M. Basheer, K. T. V. Grattan, T. Sun, A. E. Long, D. McPolin, and W. Xie, Fibre optic chemical sensor systems for monitoring pH changes in concrete,   Advanced Environmental, Chemical, and Biological Sensing Technologies, 2004, pp. 144-153.

[22]   N. Dantan, W. R. Habel, and O. S. Wolfbeis, Fiber optic pH sensor for early detection of danger of corrosion in steel-reinforced concrete structures, Smart Structures and Materials 2005: Smart Sensor Technology and Measurement Systems, 2005, pp. 274-284.

[23]   D. Staneva and R. Betcheva, Synthesis and functional properties of new optical pH sensor based on benzo[de]anthracen-7-one immobilized on the viscose, Dyes Pigments 74 (1) (2007) 148-153.

[24]   A. S. Vasylevska, A. A. Karasyov, S. M. Borisov, and C. Krause, Novel coumarin-based fluorescent pH indicators, probes and membranes covering a broad pH range, Anal. Bioanal. Chem. 387 (6) (2007) 2131-2141.

[25]   D. F. Eaton, Reference materials for fluorescence measurement, Pure Appl. Chem. 60 (7) (1988) 1107-1114.

[26]   J. B. Birks, Fluorescence quantum yield measurements, J. Res. Nat. Bur. Stand., Sect. A 80 (3) (1976) 389-399.

[27]   D. J. Maly, F. Leonetti, B. J. Backes, D. S. Dauber, J. L. Harris, C. S. Craik, and J. A. Ellman, Expedient solid-phase synthesis of fluorogenic protease substrates using the 7-amino-4-carbamoylmethylcoumarin (ACC) fluorophore, J. Org. Chem. 67 (3) (2002) 910-915.

[28]   B. Curten, P. H. M. Kullmann, M. E. Bier, K. Kandler, and B. F. Schmidt, Synthesis, photophysical, photochemical and biological properties of caged GABA,   4-[[(2H-1-benzopyran-2-one-7-amino-4-methoxy)carbonyl]   amino] butanoic acid, Photochem. Photobiol. 81 (3) (2005) 641-648.

[29]   M. Beller and C. Bolm, Transition metals for organic synthesis, in: H. Geissler (Ed.) Transition metal-catalysed cross coupling reactions, WileyVCH, Weinheim, 1998.

[30]   F. Diederich and P. J. Stang, *Metal-catalyzed cross-coupling reactions*. Weinheim: Wiley-VCH, 1998.

[31]   N. Miyaura and A. Suzuki, Palladium-catalysed cross-coupling reactions of organoboron compounds, Chem. Rev. 95 (1995) 2457-2483.

[32] W. Grahn, P. Makedonski, J. Wichern, W. Kowalsky, and S. Wiese, Fiberoptical sensors for in-situ monitoring of moisture and pH-value in reinforced concrete, Imaging Spectrometry Vii, 2001, pp. 395-403.

[33] A. Safavi and H. Abdollahi, Optical sensor for high pH values, Anal. Chim. Acta 367 (1-3) (1998) 167-173.

[34] H. W. Xu and O. A. Sadik, Design of a simple optical sensor for the detection of concentrated hydroxide ions in an unusual pH range, Analyst 125 (10) (2000) 1783-1786.

[35] F. R. Zaggout, I. M. El-Nahhal, A. E.-F. A. Qaraman, and N. Al Dahoudi, Behavior of thymol blue analytical pH-indicator entrapped into sol-gel matrix, Mater. Lett. 60 (29-30) (2006) 3463-3467.

[36] O. B. Miled, H. Ben Ouada, and J. Livage, pH sensor based on a detection sol-gel layer onto optical fiber, Mater. Sci. Eng., C 21 (1-2) (2002) 183-188.

[37] A. Safavi and M. Sadeghi, Development of an optode membrane for high pH values, Spectrochim. Acta, Part A 66 (3) (2007) 575-577.

[38] S. Miljanic and Z. Cimerman, Application of a novel lipophilized derivative of rhodamine 19 in an optical sensor suitable for measurements of pH in alkaline regions, Croat. Chem. Acta 76 (3) (2003) 199-205.

[39] A. Safavi and M. Bagheri, Novel optical pH sensor for high and low pH values, Sens. Actuators, B 90 (1-3) (2003) 143-150.

[40] S. Derinkuyu, K. Ertekin, O. Oter, S. Denizalti, and E. Cetinkaya, Fiber optic pH sensing with long wavelength excitable Schiff bases in the pH range of 7.0-12.0, Anal. Chim. Acta 588 (1) (2007) 42-49.

[41] G. E. Khalil, P. Daddario, K. S. F. Lau, S. Imtiaz, M. King, M. Gouterman, A. Sidelev, N. Puran, M. Ghandehari, and C. Brueckner, meso-Tetraarylporpholactones as high pH sensors, Analyst 135 (8) (2010) 2125-2131.

[42] C. Eggeling, J. Widengren, R. Rigler, and C. A. M. Seidel, Photobleaching of fluorescent dyes under conditions used for single-molecule detection: Evidence of two-step photolysis, Anal. Chem. 70 (13) (1998) 2651-2659.

[43] K. H. Drexhage, Fluorescence efficiency of laser-dyes, J. Res. Nat. Bur. Stand., Sect. A 80 (3) (1976) 421-428.

[44] N. i. Saleh, Y. A. Al-Soud, and W. M. Nau, Novel fluorescent pH sensor based on coumarin with piperazine and imidazole substituents, Spectrochim. Acta, Part A 71 (3) (2008) 818-822.

[45] T. Fujii, A. Ishii, Y. Kurihara, and M. Anpo, Multiple fluorescence-spectra of fluorescein molecules encapsulated in the silica xerogel prepared by the sol-gel reaction, Res. Chem. Intermediat. 19 (4) (1993) 333-342.

[46] S. T. Lee, J. Gin, V. P. N. Nampoori, C. P. G. Vallabhan, N. V. Unnikrishnan, and P. Radhakrishnan, A sensitive fibre optic pH sensor using multiple sol-gel coatings, J. Opt. A: Pure Appl. Opt. 3 (5) (2001) 355-359.

[47] F. J. Arregui, M. Otano, C. Fernandez-Valdivielso, and I. R. Matias, An experimental study about the utilization of Liquicoat solutions for the fabrication of pH optical fiber sensors, Sens. Actuators, B 87 (2) (2002) 289-295.

[48] J. Goicoechea, C. R. Zamarreno, I. R. Matias, and F. J. Arregui, Optical fiber pH sensors based on layer-by-layer electrostatic self-assembled Neutral Red, Sens. Actuators, B 132 (1) (2008) 305-311.

[49]   Y. Egawa, R. Hayashida, and J. I. Anzai, Multilayered assemblies composed of brilliant yellow and poly(allylamine) for an optical pH sensor, Anal. Sci. 22 (8) (2006) 1117-1119.

[50]   A. A. Ensafi and A. Kazemzadeh, Optical pH sensor based on chemical modification of polymer film, Microchem. J. 63 (3) (1999) 381-388.

[51]   Y. Kostov, S. Tzonkov, L. Yotova, and M. Krysteva, Membranes for optical pH sensors, Anal. Chim. Acta 280 (1) (1993) 15-19.

[52]   C. Munkholm, D. R. Walt, F. P. Milanovich, and S. M. Klainer, Polymer Modification of Fiber Optic Chemical Sensors as a Method of Enhancing Fluorescence Signal for pH Measurement, Anal. Chem. 58 (7) (1986) 1427-1430.

[53]   Z. Zhujun, Y. Zhang, M. Wangbai, R. Russell, Z. M. Shakhsher, C. L. Grant, W. R. Seitz, and D. C. Sundberg, Polyvinyl-Alcohol) as a Substrate for Indicator Immobilization for Fiber-Optic Chemical Sensors, Anal. Chem. 61 (3) (1989) 202-205.

[54]   J. Lin, Recent development and applications of optical and fiber-optic pH sensors, Trac-Trend. Anal. Chem. 19 (9) (2000) 541-552.

[55]   G. J. Mohr and O. S. Wolfbeis, Optical sensors for a wide pH range based on azo dyes immobilized on a novel support, Anal. Chim. Acta 292 (1-2) (1994) 41-48.

[56]   D. A. Nivens, Y. K. Zhang, and S. M. Angel, A fiber-optic pH sensor prepared using a base-catalyzed organo-silica sol-gel, Anal. Chim. Acta 376 (2) (1998) 235-245.

[57]   H. D. Duong, O. J. Sohn, H. T. Lam, and J. I. Rhee, An optical pH sensor with extended detection range based on fluoresceinamine covalently bound to sol-gel support, Microchem. J. 84 (1-2) (2006) 50-55.

[58]   A. Safavi and M. Pakniat, Length of stain detector for high alkalinity measurement, Anal. Lett. 31 (8) (1998) 1297-1310.

[59]   Y. A. Al-Soud, H. H. Al-Sa'doni, H. A. S. Amajaour, K. S. M. Salih, M. S. Mubarak, N. A. Al-Masoudi, and I. H. Jaber, Synthesis, characterization and anti-HIV and antitumor activities of new coumarin derivatives, Z. Naturforsch., B: Chem. Sci. 63 (1) (2008) 83-89.

[60]   Y. D. Cao, Q. Y. Zheng, C. F. Chen, and Z. T. Huang, A new fluorescent chemosensor for transition metal cations and on/off molecular switch controlled by pH, Tetrahedron Lett. 44 (25) (2003) 4751-4755.

[61]   T. H. Nguyen, T. Venugopalan, T. Sun, and K. T. V. Grattan, Development of intrinsic optical fiber pH sensors for industrial applications, in *IEEE Sensors*, vol. 1-3, 2009, pp. 89-94.

[62]   N. Opitz and D. W. Lübbers, New fluorescence photometrical techniques for simultaneous and continuous measurements of ionic strength and hydrogen ion activities, Sens. Actuators, B 4 (1983) 473-479.

Biographies

T. Hien Nguyen received the B.Sc degree in chemistry from the Vietnam National University, Hanoi, Vietnam, in 2002. She obtained the M.Sc degree in geochemistry in 2003 and the PhD degree in chemistry in 2007, from the University of Leeds, Leeds, UK. Afterwards, she became a Research Fellow in advanced chemical sensing in the School of Engineering and Mathematical Sciences, City University, London, UK until the end of 2012. She is currently working as a Research Fellow at the Organic Semiconductor Centre, University of St Andrews, St Andrews, UK. Her research interests are in the field of optical fibre sensors, molecular recognition, molecularly imprinted polymers and conjugated polymers.

Thillainathan Venugopalan received B.Eng. (Hons) degree in computer systems engineering and PhD in measurements and instrumentation from the Division of Electrical, Electronics and Information Engineering, SEMS, City University, London, U.K., in 2002 and 2008 respectively. He is currently working as an optical engineer in an optical fibre sensor company in the UK.

Tong Sun received the B.E., M.E., and Dr. Eng. degrees in mechanical engineering from the Department of Precision Instrumentation, Harbin Institute of Technology, Harbin, China, in 1990, 1993, and 1998, respectively. She received the Doctor of Philosophy degree from City University, London, U.K., in applied physics, in 1999. From 2000 to 2001, she was an Assistant Professor at Nanyang Technological University, Singapore. In 2001, she joined City University as a Lecturer. Subsequently, she was promoted to a Senior Lecturer in 2003, a Reader in 2006, and a Professor in 2008 at City University.

Kenneth T. V. Grattan graduated with a degree in physics from Queen's University, Belfast, with a B.Sc. (First Class Hon.) in 1974 and a Ph.D. degree in laser physics. He received the D.Sc. degree from City University, London, U.K., in 1992, for his sensor work. In 1978, he became a Research Fellow at the Imperial College of Science and Technology, sponsored by the Rutherford Laboratory to work on advanced photolytic drivers for novel laser systems. He joined City University in 1983 as a "new blood" Lecturer in Physics, being appointed Professor of Measurement and Instrumentation in 1991, and Head of the Department of Electrical, Electronic and Information Engineering. He is Dean of the School of Engineering and Mathematical Sciences and also Dean of the School of Informatics, City University. His research interests also include the use of fibre-optic and optical systems in the measurement of a range of physical and chemical parameters. He is the author and coauthor of over 600 publications in major international journals and at conferences and is the coeditor (with Prof. B. T. Meggitt) of a five volume topical series on *Optical Fibre Sensor Technology*.
Prof. Grattan was elected Fellow of the Royal Academy of Engineering in 2008.

Su E. Taylor is a Senior Lecturer in the School of Planning, Architecture and Civil Engineering at Queen's University of Belfast (QUB), Belfast, U.K. Her first appointment at QUB was as a Research Assistant on an EPSRC funded project which involved the use of novel internal strain gauges in steel reinforcing bars, and then she

went onto to complete another EPSRC funded project which investigated compression membrane action in high strength concrete in bridge deck slabs (GR/K57138) and received the Ph.D. degree in this area in 2000.

In 2000, she undertook a post as a Research Engineer with NITC at QUB carrying specialist R&D for the construction industry.

Dr. Taylor has been awarded two Young Researcher's Grants by the Institution of Structural Engineers (U.K.).

P.A. Muhammed Basheer, Chair of Structural Materials and Director of the Centre for Built Environment Research at Queen's University Belfast, Northern Ireland, United Kingdom, has been an educationalist and researcher in the field of civil (structural) engineering for more than 30 years. His research interests are primarily on the Science, Technology and Performance of Structural Materials, with special emphasis on non-destructive evaluation, structural health monitoring and performance testing of concrete structures. He is an elected Fellow of the Irish Academy of Engineering, Institution of Civil Engineers and American Concrete Institute. He is also a member of numerous technical committees of both the American Concrete Institute and RILEM. He has authored more than 350 technical publications.

Figure legends

Fig. 1. Experimental set-up used in the evaluation of the performance of the probe designed.

Scheme 1. Preparation of fluorescent monomers. (a) ClCOOEt, EtOAc, 100 $^{\circ}$C, 93%; (b) ethyl 4-chloroacetoacetate, H_2SO_4, H_2O, r.t, 19 h, 71%: (c) conc.H_2SO_4, glacial AcOH, 125 $^{\circ}$C, 2 h, 87%; (d) NaH (60%), 2-methyl-4-nitroimidazole, DMF, 100 $^{\circ}$C to 60 $^{\circ}$C, 18 h, 87%; (e) vinylbenzylchloride, K_2CO_3, KI, MeCN, 80 $^{\circ}$C, 2 days, 10%.

Fig.2. Absorption (left) and emission (right) spectra of **VIC** (**5**) (5 μM) in H_2O. Emission spectra recorded with $\lambda_{ex} = 370$ nm.

Scheme 2. Protonation-deprotonation equilibria of the fluorescent dye in aqueous solution

Fig. 3. Forward and reverse dynamic response of the pH sensor in the pH 10-13 range, showing the 50 minutes response time (to 95%) (($\lambda_{ex} = 375$ nm, $\lambda_{em} = 500$ nm).

Fig. 4. The evolution of fluorescence spectra of the sensor probe with pH in the range from 9.0 to 13.2. Inset shows the titration plots at 495 nm. Error bars represent standard deviations in the calculated values.

Fig. 5. Effect of ionic strength (IS) on fluorescence intensity and calculated pH value. Fluorescence intensities are normalised to the maximum emission at 495 nm of the probe at pH 10 with IS = 0.

Fig. 6. Titration plots for the sensor probe obtained the first time, after 1.5 months and after 5 months ($\lambda_{ex} = 375$ nm). Fluorescence intensities are normalised to the maximum emission at 495 nm of the probe at pH 10 for each data set. The model fits are shown in continuous lines. Error bars represent standard deviations in the calculated values.

Fig.7. Fluorescence intensity of the sensor probe (in dry state and in pH 10 buffer solution) as function of time during 60 min of continuous illumination by light from a high power Xe lamp ($\lambda_{ex} = 375$ nm, $\lambda_{em} = 500$ nm). Fluorescence intensities are normalised to the initial emission of the probe for each data set.

Mini-spectrometer

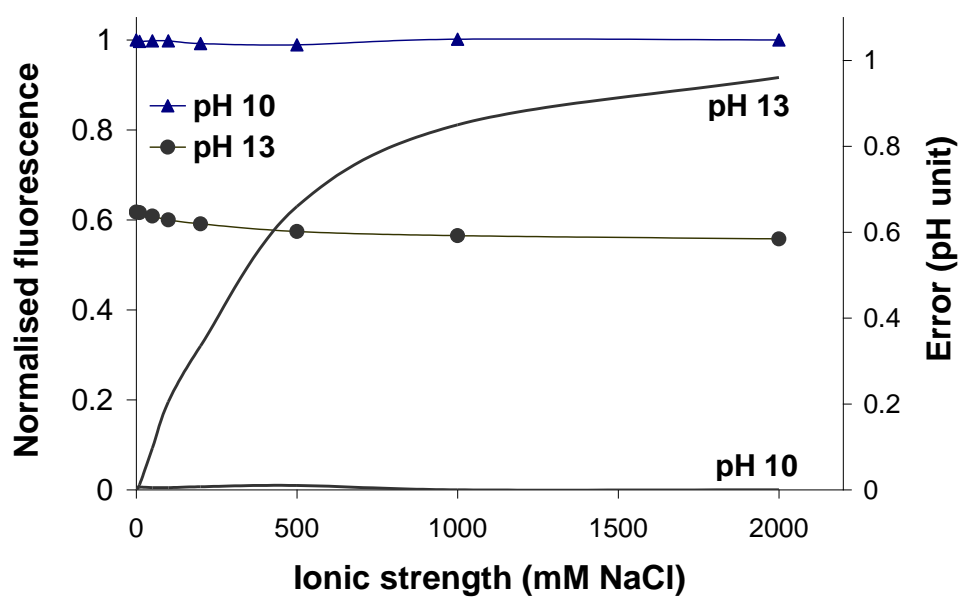Focusing lens

Collimating lens

1x2 optical fiber coupler

pH probe

LED light source

quartz disc

polymer powder

nylon membrane

sensing tablet

sensing tablet in holder

sealed holder

SMA connector

Fig. 2

Fig. 3

Fig.4

Fig.5

Fig. 6

Fig. 7